9 PRELIMINARY AGES FROM COSMOGENIC NUCLIDE BURIAL DATING OF STRATIGRAPHY IN THE MEGALOPOLIS BASIN

Mirjam Schaller[1,2,*], Todd A. Ehlers[2], Vangelis Tourloukis[3,4], Eleni Panagopoulou[5], Panagiotis Karkanas[6], Katerina Harvati[3]

[1]*Department of Geosciences, Eberhard Karls University of Tübingen, Tübingen, Germany*
[2]*School of Geographical and Earth Sciences, University of Glasgow, Glasgow, United Kingdom*
[3]*Paleoanthropology, Institute of Archaeological Sciences and Senckenberg Centre for Human Evolution and Palaeoenvironment, Department of Geosciences, Eberhard Karls University of Tübingen, Tübingen, Germany*
[4]*Department of History and Archaeology, School of Philosophy, University of Ioannina, Ioannina, Greece*
[5]*Hellenic Ministry of Culture, Ephorate of Paleoanthropology–Speleology, Athens, Greece*
[6]*M.H. Wiener Laboratory for Archaeological Science, American School of Classical Studies at Athens, Athens, Greece*
**mirjam.schaller@glasgow.ac.uk*

http://dx.doi.org/10.15496/publikation-97660

Keywords: Megalopolis Basin; burial dating; cosmogenic nuclides

9.1 INTRODUCTION

The Megalopolis Basin, an intra-mountain depression in the Central Peloponnese (Greece), consists of Pliocene–Pleistocene lacustrine and fluvial sediments. The Choremi Formation, which contains several archaeological sites of interest (e.g., Panagopoulou et al., 2018), dates to the Early and Middle Pleistocene (van Vugt et al., 2000). However, numerical dating of Middle Pleistocene lacustrine and fluvial sediments is challenging (Rixhon et al., 2017). Commonly used dating methods have a limited age range (e.g., ^{14}C dating) or are restricted due to a paucity of datable material (e.g., teeth). An intensively studied and numerically dated archaeological site in the Megalopolis Basin is Marathousa-1 (Fig. 1). Relative correlations of Marathousa-1 put the sedimentary deposits into glacial Marine Isotope Stages (MIS). Possible scenarios from relative correlations suggest sediment deposition during MIS 16 (Van Vugt et al., 2000) as well as MIS 14, or possibly MIS 12 (Okuda et al., 2002; Tourloukis et al., 2018). Numerical age dating of the sediment with pIRIR on K-Feldspar reflects a deposition during MIS 12 (Jacobs et al., 2018), although these samples are near, or at, a saturation of this technique and could represent minimum ages. In contrast, a cervid molar from the artifact- and fossil-bearing unit dated with ESR indicates a deposition age during MIS 13 and a maximum age during MIS 16 (Blackwell et al., 2018). Neither relative nor numerical dating give a conclusive answer of the depositional age for archaeological findings at the Marathousa-1 site.

M. Schaller: https://orcid.org/0000-0003-2722-9537
T. A. Ehlers: https://orcid.org/0000-0001-9436-0303
V. Tourloukis: https://orcid.org/0000-0002-9527-2708
E. Panagopoulou: https://orcid.org/0000-0002-4268-6157
P. Karkanas: https://orcid.org/0000-0002-7156-671X
K. Harvati: https://orcid.org/0000-0001-5998-4794

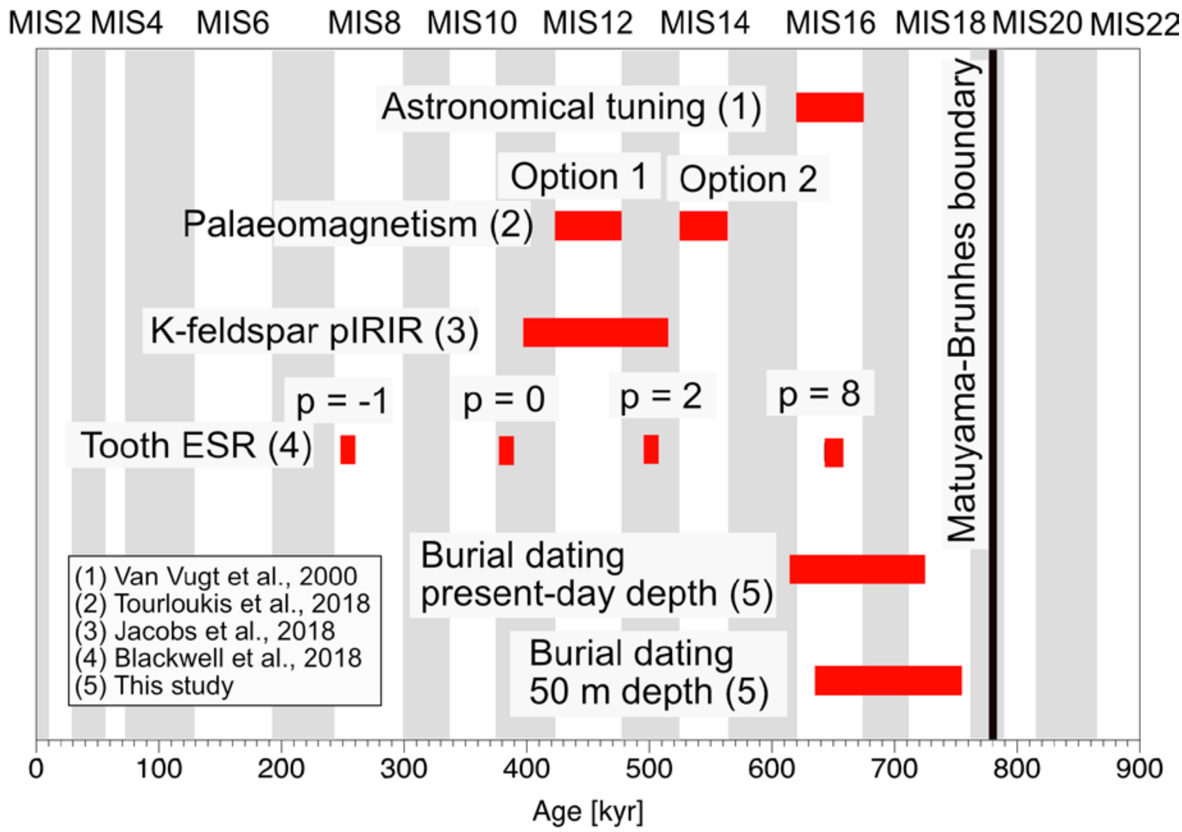

Figure 1: Compilation of relative and numerical deposition age ranges for Marathousa-1 (red blocks). In addition, the age of the Brunhes-Matuyama boundary and the ages of the different Marine Isotope Stages MIS are indicated. Glacial and interglacial MIS are in white and gray, respectively.

In this study, numerical ages of sediment deposits are addressed with the method of burial daring with a pair of in situ-produced cosmogenic nuclides (e.g., Granger, 2014). Some studies refer to this technique as 'simple' burial dating, in contrast to the isochron burial dating technique. The cosmogenic nuclides used here are ^{26}Al and ^{10}Be in situ-produced in quartz. The method makes use of the fact that ^{26}Al decays faster than ^{10}Be. The production rate ratio of ^{26}Al/^{10}Be in quartz during sediment production is known. Hence the measured ratio in quartz material from sediment deposits can be used to monitor the time since sediment production. Under the assumption that sediment transport time is short in comparison to burial time, the sediment deposition age can be determined. Four samples from Marathousa-1 and three from Tripotamos-4 were analyzed and deposition ages were calculated.

9.2 STUDY AREAS AND SAMPLING LOCATIONS

The Megalopolis Basin formed during the Late Miocene–Pliocene times and contains Pliocene–Pleistocene lacustrine and fluvial deposits of more than 250 m thickness (Vinken, 1965). These deposits have previously been divided into six formations, of which the Choremi formation is of interest. In the deposits of this formation, the archaeological sites Marathousa-1 and Tripotamos-4 were investigated with in situ-produced cosmogenic nuclides.

9.2.1. MARATHOUSA-1

The Lower Palaeolithic site Marathousa-1 is located at ~350 m above mean sea level and is exposed inside one of the lignite mines (also called Marathousa Mine) at the center-west part of the basin. Paleoanthropological material was found in lacustrine deposits with clay, silt, and sand, which are sandwiched between the lignite seam II and III. The detrital sediments were sampled for cosmogenic nuclide analysis at Martahousa-1A in the stratigraphic layer UA3b (Table 1) directly overlying the artifact-bearing horizon (UA3c/UA4, see Karkanas et al., 2018). In Marathousa-1B, two samples were collected from the stratigraphic layer UB4a and in the lowermost part of UB9. Samples from the stratigraphic layers UA3b and UB4a were very clay-rich. Only a small amount and fine-grained quartz was recovered, making the application of cosmogenic nuclide burial dating difficult. In contrast, more and coarser-grained quartz was separated from the stratigraphical layer UB9.

9.2.2. TRIPOTAMOS-4

The archaeological site of Tripotamos-4 was found in the area east of the village of Tripotamos. Two survey units (4 and 5) were examined more closely in 2020. The deposits are stratigraphically placed into, but most likely lie above, the lignite seam III (Löhnert and Nowack, 1965). At this location, lacustrine, bluish grey clayey deposits, poor in organic material, are laterally interfingered with fluvial/fluvio-lacustrine deposits of yellow sandy silts and intercalated layers of coarser grained sands and gravels. Sediment samples from survey unit 4 were collected from a layer of yellow sands of terrestrial origin for dating with in situ-produced cosmogenic nuclides.

Stratigraphic layer	Sample ID	Location (WGS 84)		Altitude	Excavation square	Present-day Overburden		
		°N Latitude	°E Longitude	m			m	
Marathousa-1								
UA3b	CN-UA3b-1	37,40833	22,09147	349.51	940/671	30	±	3
UA3b	CN-UA3b-2	37,40833	22,09147	349.51	940/669	30	±	3
UB4a	CN-UB4a-1	37,40833	22,09147	350.85-350.65	934/610	30	±	3
UB9, lowermost part	CN-UB9-1	37,40833	22,09147		East Section	30	±	3
Tripotamos-4								
	TRP Cosmo 1	37,3589	22,10722	394,8		7	±	1
	TRP Cosmo 2	37,3589	22,10722	394,8		7	±	1
	TRP Cosmo 3	37,3589	22,10722	394,8		7	±	1

Table 1: Sample location and information.

9.3 BURIAL DATING METHOD

Pairs of in situ-produced cosmogenic nuclides analyzed in quartz sediment can be used for burial dating based on different decay rates of two isotopes measured in the same sample material (e.g., Granger et al., 1997; Granger and Muzikar, 2001). Age determination of sediment deposition in the two study areas makes use of minimum and maximum burial ages with in situ-produced ^{26}Al and ^{10}Be concentrations in quartz (e.g., Granger, 2014). A minimum burial age is calculated based on the sample specific $^{26}Al/^{10}Be$ ratio and the assumption of no post-burial irradiation due to deep burial (e.g., 50 m). In contrast, using the present-day sample depth will result in a maximum burial age. As sediment overburden may have diminished over time (e.g., due to post-depositional erosion), the "real" age of the sediment deposit is bracketed by the minimum and maximum ages.

Samples from Marathousa-1A and 1B were collected from different depths, whereas samples collected in Tripotamos-4 were from the same stratigraphic depth. After washing and sieving the samples, quartz was separated and cleaned to reach Al-concentrations in quartz as low as possible (goal <100 ppm). Al and Be were extracted according to protocols outlined in Schaller et al. (2016). $^{26}Al/^{27}Al$ and $^{10}Be/^{9}Be$ ratios of samples, blanks, and standards were measured at the AMS facility of Cologne (Dewald et al., 2013). ^{26}Al and ^{10}Be concentrations of samples were corrected for chemistry blanks (Table 2). ^{27}Al concentrations were measured with standard addition on an ICP-OES at the University of Tübingen.

Minimum and maximum burial ages were determined with a MatLab script modified from Schaller et al. (2016). Decay constants used for ^{26}Al and ^{10}Be were (9.830 ± 0.250) x10^{-7} (see Norris et al., 1983) and (4.997 ± 0.043) x10^{-7} (Chmeleff et al., 2010; Korschinek et al., 2010). Sea level-high latitude (SLHL) production rates for ^{26}Al are 28.54, 0.84, and 0.081 atoms/(g(qtz) yr) for nucleonic, stopped muonic, and fast muonic production, respectively (Borchers et al., 2016; Braucher et al., 2011). The SLHL production rates are 3.92, 0.012, and 0.039 atoms/(g(qtz) yr) for nucleonic, stopped muonic, and fast muonic ^{10}Be production, respectively (Borchers et al., 2016; Braucher et al., 2011). The $^{26}Al/^{10}Be$ ratio of production at SLHL is ~7.4. SLHL production rates are scaled to the sample location with the online calculator of Marrero et al. (2016) using the scaling procedure "SA" based on Lifton et al. (2014). Production rates at the sampling depths were calculated based on nucleonic, stopped muonic, and fast muonic adsorption lengths, which are 157, 1500, and 4320 g/cm^2, respectively (Braucher et al., 2011). The density of the overburden was assumed to be constant over time with a value of 2.0 ± 0.1 g/cm^3. As the production rates of the sediment source in the past cannot be determined, the values of the production rates at the sample location were used for age calculation. This assumption results in a maximum burial age. The minimum overburden for Tripotamos-4 assumed to be 7 m and results in a maximum burial age. The original amount of sediment deposited in the study areas, as well as post-depositional erosion of sediments, are both unknown. Given this uncertainty, a second burial age was calculated with the assumption of an initial (depositional) overburden of 50 m, that would have been eroded post-depositional in the recent past. This second approach (50 m of original overburden) provides the sensitivity of the burial ages reported here to changing depositional conditions.

Table 2: Cosmogenic nuclide information.

Strati-graphic layer	Sample ID	Grain size µm	Qtz dis-solved g	Qtz ^{27}Al conc. ppm	^{26}Al/^{27}Al	Error %	^{26}Al conc. 10^4 atoms/g(qtz)	m(^{9}Be) mg	^{10}Be/^{9}Be	Error %	^{10}Be conc. 10^4 atoms/g(qtz)	^{26}Al/^{10}Be	Burial dating present-day depth kyr	Burial dating 50 m depth kyr
Marat-housa-1 a)													(30 m depth)	(50 m depth)
UA3b	CN-UA3b-1	125-250	68,47	374	4,03E-14	7,45	33,62 ± 2,51	0,29	2,29E-13	4,30	6,36 ± 0,28	5,28 ± 0,46	642 ± 98	674 ± 100
UA3b	CN-UA3b-2	125-250	72,43	389	3,85E-14	6,81	33,40 ± 2,28	0,29	2,50E-13	4,08	6,59 ± 0,27	5,07 ± 0,40	725 ± 92	758 ± 94
UB4a	CN-UB4a-1	125-1000	11,34	515	4,85E-14	6,59	55,40 ± 3,68	0,29	6,21E-14	4,64	10,20 ± 0,50	5,43 ± 0,45	609 ± 96	627 ± 98
UB9, lowermost part	CN-UB9-1	250-500	75,93	156	1,44E-13	4,20	50,08 ± 2,11	0,29	3,83E-13	3,45	9,64 ± 0,33	5,20 ± 0,28	702 ± 66	723 ± 68
												mean ± stdev	670 ± 53	696 ± 57
Tripo-tamos-4 b)													(7 m depth)	(50 m depth)
Unit4	TRP Cosmo 1	250-500	39,72	108	1,74E-13	4,57	41,87 ± 2,73	0,34	1,33E-13	3,8	7,64 ± 0,32	5,48 ± 0,43	1180 ± 238	611 ± 95
Unit4	TRP Cosmo 2	250-500	39,83	122	1,67E-13	4,73	45,41 ± 2,84	0,34	1,23E-13	3,9	7,05 ± 0,30	6,44 ± 0,49	467 ± 173	278 ± 90
Unit4	TRP Cosmo 3	250-500	39,58	111	1,68E-13	4,49	41,57 ± 2,64	0,34	1,28E-13	3,8	7,36 ± 0,31	5,65 ± 0,43	1046 ± 225	548 ± 93
												mean ± stdev	898 ± 379	479 ± 177

a) The ^{26}Al and ^{10}Be concentrations are corrected with a chemistry blank of 44129 ±8045 atoms and 35521 ±11511 atoms, respectively.

The nucleonic, stopped and fast muonic production rates at sample location for ^{26}Al are 25.211 atoms/(g(qtz)*yr), 0.799 atoms/(g(qtz)*yr), and 0.077 atoms/(g(qtz)*yr), respectively.

The nucleonic, stopped and fast muonic production rates at sample location for ^{10}Be are 3.518 atoms/(g(qtz)*yr), 0.011 atoms/(g(qtz)*yr), and 0.037 atoms/(g(qtz)*yr), respectively.

b) For the ^{26}Al concentrations there is no chemistry blank detected. The ^{10}Be concentrations were corrected with 23017 ±15063 atoms, respectively.

The nucleonic, stopped and fast muonic production rates at sample location for ^{26}Al are 26.152 atoms/(g(qtz)*yr), 0.819 atoms/(g(qtz)*yr), and 0.079 atoms/(g(qtz)*yr), respectively.

The nucleonic, stopped and fast muonic production rates at sample location for ^{10}Be are 3.651 atoms/(g(qtz)*yr), 0.012 atoms/(g(qtz)*yr), and 0.038 atoms/(g(qtz)*yr), respectively.

9.4 RESULTS

9.4.1. MARATHOUSA-1

In situ-produced cosmogenic nuclide concentrations of ^{26}Al and ^{10}Be for the replicate samples from Marathousa-1A are (33.62 ±2.51) and (33.40 ±2.28) x10^4 atoms/g(qtz) and (6.36 ±0.28) and (6.59 ±0.27) x10^4 atoms/g(qtz), respectively (Table 2). ^{26}Al/^{10}Be ratios are 5.28 ±0.46 and 5.07 ±0.40 for the two replicate samples. Based on the present-day sample depth of 30 m, these ratios result in burial ages of 642 ±98 kyr and 725 ±92 kyr.

Two samples from Marathousa-1B collected from a different sample location show in situ-produced cosmogenic nuclide concentrations of ^{26}Al and ^{10}Be of (55.40 ±3.68) and (55.08 ±2.11) x10^4 atoms/g(qtz) and (10.20 ±0.50) and (9.64 ±0.33) x10^4 atoms/g(qtz), respectively (Table 2). The two samples have ^{26}Al/^{10}Be ratios of 5.43 ±0.45 and 5.20 ±0.28. The burial ages based on the present-day sampling depth of 30 m are 609 ±96 kyr and 702 ±67 kyr.

9.4.2. TRIPOTAMOS-4

In situ-produced cosmogenic nuclide concentrations of ^{26}Al and ^{10}Be for the three samples range from (41.57 ±2.64) to (45.41 ±2.84) x10^4 atoms/g(qtz) and (7.05 ±0.30) to (7.64 ±0.32) x10^4 atoms/g(qtz), respectively (Table 2). ^{26}Al/^{10}Be ratios are 5.48 ±0.43, 6.44 ±0.49, and 5.65 ±0.43 for the three samples from the same stratigraphic layer. Based on the sampling depth of 7 m below the present-day surface, these ratios result in burial ages of 1180 ±238 kyr, 467 ±173 kyr, and 1046 ±225 kyr. Based on a constant burial depth of 50 m, the ages are 611 ±95 kyr, 278 ±90 kyr, and 548 ±93 kyr, respectively.

9.5 DISCUSSION

9.5.1. MARATHOUSA-1 AND TRIPOTAMOS-4

The four analyzed samples from Marathousa-1 resulted in burial ages ranging from 609 ±96 kyr to 725 ±92 kyr. The large errors in the ages result from uncertainties in the cosmogenic nuclide concentrations as well as the propagation of these errors in the age calculation. Additional analytical problems were caused by the restricted sample amount as well as the cleanness of the quartz (e.g., ^{27}Al concentration). Nevertheless, the four samples report minimum burial ages that agree with each other within error (Table 2). The resulting mean minimum burial age is 670 ±53 kyr putting the sediment layer between lignite seam II and III within MIS 16 (Fig. 1). An assumption made and influencing the burial age is the cosmogenic production rate in the sediment production area. A best guess of a value for this production rate is the production rate of the sample location. As this production rate is a minimum value, the resulting age is a maximum burial age. Unfortunately, neither the production rates in the sediment source nor the burial depth over time can be completely evaluated. Therefore, the herein reported burial age is considered a best estimate possible with this technique.

The Tripotamos-4 location has similar uncertainties with the calculated burial ages. Even though there was enough and well-cleaned sample material available, the calculated ages from the three samples collected at 7 m depth are highly variable. One sample does not even agree within error with the other two samples. In addition, the sampling depth of 7 m is insufficient to avoid post-depositional irradiation and nuclide production. Due to this, the burial age based on 7 m of overburden should be considered as the maximum age because if (as is likely) additional overburden was present in the past, then the age would be younger than this 7 m overburden estimate. Assuming that the samples were covered with 50 m overburden over most of the time, the mean burial age is 479 ±177 ky. However, the sediment deposit cannot be attributed to a MIS, only the relative stratigraphy is maintained, and the numerical age of the archaeological site Tripotamos-4 remains vague.

9.6 CONCLUSIONS

The archaeological site of Marathousa-1 has been attributed with relative and numerical dating techniques to MIS12. However, the cosmogenic nuclide-based new mean burial age from Marathousa-1 of 670 ±53 kyr suggests that the site could belong to MIS16. Unfortunately, such an age determination does not match well with the rest of the chronological evidence based on both site- and basin-scale chronostratigraphic constraints (Tourloukis et al., 2018 and references therein). Samples from Tripotamos-4 could not be used to date the deposit above lignite seam III. The mean burial age based on the three samples and assuming a constant overburden of 50 m resulted in an age of 479 ±177 kyr showing a large error due to highly variable age constraints. Therefore, considering the error margin of this assessment, the attribution of Tripotamos-4 to a MIS is not possible based on the available data.

ACKNOWLEDGMENTS

This research was conducted under a permit granted to the Ephorate of Palaeoanthropology-Speleology, Hellenic Ministry of Culture. It was supported by the ERC Consolidator Grant ERC-CoG-724703 (“CROSSROADS”) and the ERC Starting Grant ERC-StG-283503 (“PaGE”), both awarded to K.H. K.H. is also supported by the ERC Advanced Grant ERC-AdG-101019659 (“FIRSTSTEPS”). We would like to thank G. Rixhon and an anonymous reviewer for their input and improvement of the extended abstract.

REFERENCES

Blackwell B.A.B., Sakhrani, N., Singh, I.K., Gopalkrishne, K.K., Tourloukis, V., Panagopoulou, E., Karkanas, P., Blickstein, J.I.B., Skinner, A.R., Florentin, J.A. and Harvati, K. 2018. ESR Dating Ungulate Teeth and Molluscs from the Paleolithic Site Marathousa 1, Megalopolis Basin, Greece, Quaternary, 1, 22.

Borchers, B., Marrero, S., Balco, G., Caffee, M., Goehring, B., Lifton, N., Nishiizumi, K., Phillips, F., Schaefer, J. and Stone, J., 2016. Geological calibration of spallation production rates in the CRONUS-Earth project. Quaternary Geochronology, 31, pp. 188–198.

Braucher, R., Merchel, S., Borgomano, J. and Bourlès, D.L., 2011. Production of cosmogenic radionuclides at great depth: A multi element approach. Earth and Planetary Science Letters, 309, pp. 1–9.

Chmeleff, J., von Blanckenburg, F., Kossert, K. and Jakob, D., 2010. Determination of the 10Be half-life by multicollector ICP-MS and liquid scintillation counting. Nuclear Instruments and Methods in Physics Research Section B: Beam Interactions with Materials and Atoms, 268, pp. 192–199.

Dewald, A., Heinze, S., Jolie, J., Zilges, A., Dunai, T., Rethemeyer, J., Melles, M., Staubwasser, M., Kuczewski, B., Richter, J., Radtke, U., von Blanckenburg, F. and Klein, M., 2013. Cologne AMS, a dedicated center for accelerator mass spectrometry in Germany. Nuclear Instruments and Methods in Physics Research Section B: Beam Interactions with Materials and Atoms, 294, pp. 18–23.

GRANGER, D.E., 2014. Cosmogenic Nuclide Burial Dating in Archaeology and Paleoanthropology. Treatise on Geochemistry, 14, pp. 81–97.

GRANGER, D.E. and Muzikar, P.F., 2001. Dating sediment burial with in situ-produced cosmogenic nuclides: Theory, techniques, and limitations. Earth and Planetary Science Letters, 188, pp. 269–281.

GRANGER, D.E., Kirchner, J.W. and Finkel, R.C., 1997. Quaternary downcutting rate of the New River, Virginia, measured from differential decay of cosmogenic 26Al and 10Be in cave-deposited alluvium. Geology, 25 (2), pp. 107–110.

JACOBS, Z., Li, B., Karkanas, P., Tourloukis, V., Thompson, N., Panagopoulou, E. and Harvati, K., 2018. Optical dating of K-feldspar grains from Middle Pleistocene lacustrine sediment at Marathousa 1 (Greece), Quaternary International, 497, pp. 170–177.

KARKANAS, P., Tourloukis, V., Thompson, N., Giusi, D., Panagopoulou, E. and Harvati, K., 2018. Sedimentology and micromorphology of the Lower Palaeolithic lakeshore site Marathousa 1, Megalopolis Basin, Greece. Quaternary International, 497, pp. 123–136.

KORSCHINEK, G., Bergmaier, A., Faestermann, T., Gerstmann, U.C., Knie, K., Rugel, G., Wallner, A., Dillmann, I., Dollinger, G., von Gostomski, C.L., Kossert, K., Maiti, M., Poutivtsev, M. and Remmert, A., 2010. A new value for the half-life of 10Be by Heavy-Ion Elastic Recoil Detection and liquid scintillation counting. Nuclear Instruments and Methods in Physics Research Section B: Beam Interactions with Materials and Atoms, 268, pp. 187–191.

LIFTON, N., Sato, T., Dunai, T., 2014. Scaling in situ cosmogenic nuclide production rates using analytical approximations to atmospheric cosmic-ray fluxes. Earth and Planetary Science Letters, 386, pp. 149–160.

LÖHNERT, E. and Nowak, H., 1965. Die Braunkohlenlagerstätte von Khoremi im Becken von Megalopolis. Peloponnes. Geologisches Jahrbuch, 82, pp. 84–-868.

MARRERO, S.M., Phillips, F.M., Borchers, B., Lifton, N., Aumer, R. and Balco, G., 2016. Cosmogenic nuclide systematics and the CRONUScalc program. Quaternary Geochronology, 31, pp. 160–187.

NORRIS, T.L., Gancarz, A.J., Rokop, D.J. and Thomas, K.W., 1983. Half-life of 26A1. Lunar Planet. Sci. Conf., Journal of Geophysical Research, 88, B331–B333.

OKUDA, M., van Vugt, N., Nakagawa, T., Ikeya, M., Hayashida, A., Yusada, Y. and Setoguchi, T., 2002. Palynological evidence for the astronomical origin of lignite-detritus sequences in the Middle Pleistocene Marathousa Member, Megalopolis, SW Greece. Earth and Planetary Science Letters, 201, pp. 143–157.

PANAGOPOULOU, E., Tourloukis, V., Thompson, N., Konidaris, G., Athanassiou, A., Giusti, D., Tsartsidou, G., Karkanas, P. and Harvati, K., 2018. The Lower Palaeolithic site of Marathousa 1, Megalopolis, Greece: Overview of the evidence. Quaternary International, 497, pp. 33–46.

RIXHON, G., Briant, R., Cordier, S., Duval, M., Jones, A. and Scholz, D., 2017. Revealing the pace of river landscape evolution during the Quaternary: Recent developments in numerical dating methods. Quaternary Science Reviews, 166, pp. 91–113.

SCHALLER, M., Ehlers, T. A., Stor, T., Torrent, J., Lobato, L., Christl, M. and Vockenhuber, C., 2016. Timing of European fluvial terrace formation and incision rates constrained by cosmogenic nuclide dating. Earth and Planetary Science Letters, 451, pp. 221–231.

TOURLOUKIS, V., Muttoni, G., Karkanas, P., Monesi E., Scardia, G., Panagopoulou, E. and

Harvati, K., 2018. Magnetostratigraphic and chronostratigraphic constraints on the Marathousa 1 Lower Palaeolithic site and the Middle Pleistocene deposits of the Megalopolis Basin, Greece, Quaternary International, 497, pp. 154–169.

Van Vugt, N., de Bruijn, H., van Kolfschoten, M. and Langereis, C.G., 2000. Magneto- and cyclostratigraphy and mammal-fauna's of the Pleistocene lacustrine Megalopolis Basin, Peloponnesos, Greece, Geologica Ultraiectina, 189, pp. 69–92.

Vinken, R., 1965. Stratigraphie und Tektonik des Beckens von Megalopolis (Peloponnes, Griechenland). Geol. Jahrb., 83, pp. 97–148.